Hindawi
Journal of Chemistry
Volume 2023, Article ID 9768184, 1 page
https://doi.org/10.1155/2023/9768184

Retraction

Retracted: Mechanical Performance Analysis of Steel Beam-Column Joints in Fabricated Multirise Steel Structures after Fire

Journal of Chemistry

Received 28 November 2023; Accepted 28 November 2023; Published 29 November 2023

This article has been retracted by Hindawi, as publisher, following an investigation undertaken by the publisher [1]. This investigation has uncovered evidence of systematic manipulation of the publication and peer-review process. We cannot, therefore, vouch for the reliability or integrity of this article.

Please note that this notice is intended solely to alert readers that the peer-review process of this article has been compromised.

Wiley and Hindawi regret that the usual quality checks did not identify these issues before publication and have since put additional measures in place to safeguard research integrity.

We wish to credit our Research Integrity and Research Publishing teams and anonymous and named external researchers and research integrity experts for contributing to this investigation.

The corresponding author, as the representative of all authors, has been given the opportunity to register their agreement or disagreement to this retraction. We have kept a record of any response received.

References

[1] F. Liu, X. Wang, B. Cai, X. Li, and L. Yang, "Mechanical Performance Analysis of Steel Beam-Column Joints in Fabricated Multirise Steel Structures after Fire," *Journal of Chemistry*, vol. 2022, Article ID 7425801, 8 pages, 2022.

Hindawi
Journal of Chemistry
Volume 2022, Article ID 7425801, 8 pages
https://doi.org/10.1155/2022/7425801

Research Article

Mechanical Performance Analysis of Steel Beam-Column Joints in Fabricated Multirise Steel Structures after Fire

Fang Liu,[1,2] **Xiuli Wang**,[1,2] **Bin Cai**,[1,2] **Xuguang Li**,[1,2] **and Liqi Yang**[1,2]

[1]*School of Civil Engineering Jilin Jianzhu University, Jilin, China*
[2]*Jilin Province Zhongrun Steel Structure Technology Co.,Ltd, Jilin, China*

Correspondence should be addressed to Fang Liu; 2015080@qhnu.edu.cn

Received 26 April 2022; Revised 25 May 2022; Accepted 1 June 2022; Published 14 June 2022

Academic Editor: Aruna K K

This study aims to analyze the mechanical properties of fabricated multistory and high-rise steel structures and steel beam-column joints after fire. Considering that the steel structure building has the characteristics of good seismic resistance, flexible structural layout, short construction period, and good safety, first, the thermal and mechanical properties of steel are analyzed. They are thermal conductivity, the thermal expansion coefficient of steel, yield strength, and elastic modulus of ordinary steel. Next, the thermal conduction principle of steel under fire environment is analyzed, including thermal conduction, thermal convection, and thermal radiation. Then, the three-story and three-span reinforced concrete is selected as the experimental object. The local frame calculation model is established through the finite element software Abaqus. It is found that when the axial compression ratio is 1.0 and the fire time of the steel body is 180 min, the vertical deformation speed of the middle column and side column of the frame will increase rapidly. Besides, the bending moment at the bottom of the side column of the frame will increase inversely. The change is not obvious when the axial compression ratio is other values. The axial deformation of the universal beam is obvious under the condition of different fire load ratios. When the load ratio increases, the maximum fire resistance of the universal beam will decrease rapidly. Meanwhile, when the steel body is subjected to the same load ratio, different bearing capacity β has little effect on the fire resistance limit of the steel body. This thesis focuses on a series of changes in the steel of fabricated multistory and high-rise steel buildings after the fire, hoping to provide a reference for the relevant teams of steel construction and make the future housing construction safer.

1. Introduction

In the 18th century, steel structure buildings first appeared in Britain. Up to now, steel has become the most important building material among multiple building materials. The emergence of steel structures has changed people's understanding of building materials and changed the designer's concept of architectural design in the whole industry. Since the reform and opening up, China's scientific and technological level has developed by leaps and bounds, and the field of steel structure has also seized this development opportunity [1]. During this period, China has improved both in construction technology and production technology, making the application of steel structure in China increasingly widely. For example, Shanghai World Expo Exhibition Hall, National Stadium in Beijing, Shanghai World Financial Center, and Canton Tower represent China's application level in steel structure [2]. At present, steel structure buildings show good safety, quality, and earthquake resistance characteristics and are favored by multiple engineering enterprises. However, there are some limitations, such as poor fire resistance of steel structures [3]. The reason is that the performance of steel will decline significantly in a high-temperature environment or when a fire occurs. The yield strength of steel will change and gradually decrease when the temperature of steel structure building is above 200°C. When the temperature rises to 400°C, steel's elastic modulus and yield strength will decrease by more than 50%. If the ambient temperature rises to 600°C, the strength and stiffness of steel will be basically lost [4]. It suggests that when a fire occurs, the steel structure building is easy to be damaged if it has not been protected. According to the statistics of relevant

research teams, most steel structure buildings will be damaged as a whole within 15–20 minutes of the fire. In addition, steel buildings will also have apparent thermal expansion and cold contraction, and thermal expansion will occur in a high-temperature environment. In the fire fighting process, the steel shrinks due to the decrease of ambient temperature. Such a change will significantly change the stress state of steel, so that the steel structure building cannot meet the use requirements. At present, the rapid development of urbanization has also promoted the continuous progress of the construction industry. Under this situation, all kinds of new architectural forms come into being. Large space structures and high-rise structures have been loved and pursued by more and more people because of their unique charm. However, due to the improvement of the building function demand, the demand for other auxiliary facilities, such as power and heat, has also increased a lot. It has led to a significant increase in the potential fire hazards inside the building. In the past decades, there have been many steel structure collapse accidents caused by the fire in China.

Chan et al. studied the effects of several factors on the functionally graded concretes (FGCs) bonding quality of steel fiber and recycled aggregate in multistory and high-rise steel structure buildings. The test results show that the influence of aggregate type and casting delay between layers on the quality of layer transition zone (LTZ) in the studied FGC is greater than that of fiber content. In addition, the FGC studied can be produced when the interlayer casting delay time is less than 24 hours without losing mechanical properties, increasing the potential for large-scale production of low-bearing capacity structures [5]. Ahmad et al. studied the effects of different amounts of steel fiber on the mechanics and durability of concrete. The compressive strength and splitting tensile strength of steel structures cured for 7 and 28 days were studied. Various parameters such as water absorption, acid corrosion resistance, and permeability were studied to evaluate the durability of each mixture. The results show that the strength of the composite increases to 2% and then decreases gradually with the addition of steel fiber. When the content of steel fiber is 2.0%, the durability parameters such as water absorption, permeability, and acid corrosion resistance of concrete are significantly improved. Therefore, it is recommended to mix steel fibers at 2.0% of the weight of cement to achieve maximum benefits [6].

This thesis is to analyze the mechanical and thermal performance of steel structure and steel beam-column joints in fabricated multistory and high-rise steel structure buildings after the fire. By establishing a three-story and three-span reinforced concrete model and selecting a local frame, the deformation of its side column, middle column, and beam is analyzed. The research innovation is to analyze the steel structure joints through the combination of thermal and mechanical properties, which significantly improves the accuracy of the conclusion. It is hoped that this thesis can help relevant design teams to complete the design of steel structures better and reduce the impact of fire factors on steel structures.

2. Research Scheme Design

2.1. Performance of Semirigid Joints. Nowadays, urban life fires occur frequently, and the research on the fire resistance of steel structure buildings has become extremely important. Therefore, in steel structure buildings, it is more necessary to focus on the analysis of joint performance under fire:

(1) In a high-temperature environment, steel yield strength will gradually decrease, which will change the internal force redistribution of each joint of the steel structure. In general, the change of internal force redistribution will seriously impact steel structure buildings. If it is in a high-temperature environment for a long time, the steel structure will be seriously deformed, resulting in collapse [7].

(2) Under the action of high temperature or fire, due to the thermal expansion effect of steel, the member produces large deformation and great additional stress to the joints, resulting in joint failure.

(3) Joint is an essential component in the joint connection structure. The research on joint performance can more effectively grasp the overall performance of the structure. The research on the fire resistance performance of the joint can reduce or avoid the damage of the structure in fire or make the structure have a certain fire resistance period to ensure the safety of life and property.

2.2. Thermal Properties of Steel

2.2.1. Thermal Conductivity λ_s. Generally, the higher the temperature is, the lower the thermal conductivity of the steel itself is. When the temperature reaches a certain value, the thermal conductivity of the steel body will not change. Therefore, China has made a specified value for the thermal conductivity of the steel body:

$$\lambda_S = \frac{45W}{\left(m^2 \cdot {}^\circ C\right)}. \tag{1}$$

2.3. Specific Heat Capacity of Steel C_S. It represents the ability of the steel body to release and absorb energy. China also stipulates the value of specific heat capacity of steel body:

$$C_S = \frac{600J}{kg \cdot {}^\circ C}. \tag{2}$$

When the temperature of the steel body is higher, the specific heat capacity of the steel will also increase. When the steel temperature reaches 600°C~700°C, sudden change will occur and the specific heat capacity will decrease. The reason why the specific heat capacity of steel changes suddenly is that when the steel reaches 600°C~700°C, the crystal lattice vibration inside the steel body changes from the previous orderly movement to disordered movement, resulting in the disappearance of magnetism, and finally, the specific heat capacity of steel changes [8]. When the temperature of the

steel body increases gradually, the steel is also gradually completing the disordered transformation, so the specific heat capacity of the steel decreases.

2.3.1. Steel Density ρ_s. Steel density ρ_s will not change due to external temperature change, which is determined by the steel itself. Therefore, China uniformly sets the density of steel as $\rho_s = 7850\,\mathrm{kg/m^3}$.

2.3.2. Thermal Expansion Coefficient of Steel α_s. The coefficient of thermal expansion represents the ratio between the change of unit length of steel and the original length when the temperature of steel increases by 1°C, and its unit is m/(m•°C). When the thermal-mechanical coupling method is used to analyze the steel structure, the coefficient of thermal expansion is an essential physical quantity [9]. Although the thermal expansion coefficient α_s of steel will change with temperature to a certain extent, the overall change range is not large. Therefore, China also stipulates the value of thermal expansion coefficient of steel at high temperature:

$$\alpha_S = \frac{1.4 \times 10 - 5m}{(m \cdot {}^{\circ}C)}. \tag{3}$$

2.4. Mechanical Properties of Steel

2.4.1. Yield Strength f_y of Ordinary Steel. Steel has no yield strength at high temperature, but on the contrary, the yield strength at room temperature is apparent [10]. Therefore, China has also made a standardized definition of this:

$$\begin{aligned}
&\frac{f_{yT}}{f_y} = 120^{\circ}C \le T \le 300^{\circ}C,\\
&\frac{f_{yT}}{f_y} = 1.24 \times 10 - 8T3 - 2.096 \times 10 - 5T2 + 9.228\\
&\qquad \times 10 - 3T - 0.2168 \cdot 300^{\circ}C \le T \le 800^{\circ}C,\\
&\frac{f_{yT}}{f_y} = \frac{0.5 - T}{20000} 800^{\circ}C \le T \le 1000^{\circ}C,
\end{aligned} \tag{4}$$

where $f_{yT}/f_y = 1.24 \times 10 - 8\mathrm{T}3 - 2.096 \times 10 - 5\mathrm{T}2 + 9.228 \times 10 - 3\mathrm{T} - 0.2168$ $f_{yT}/f_y = 0.5 - \mathrm{T}/20000 f_{yT}$ represents the yield strength when the external temperature of the steel is T. f_y represents the yield strength of steel under normal temperature.

2.4.2. Elastic Modulus E of Ordinary Steel. The elastic modulus of steel will decrease obviously under high-temperature conditions, and the steel will deform obviously under the action of external load [11, 12]. Therefore. China has formulated the following specifications for the calculation of elastic modulus of ordinary steel under high-temperature conditions:

$$\begin{aligned}
&\frac{E_T}{E} = \frac{7T - 4780}{6T - 4760} \quad 20 \le T \le 600^{\circ}C,\\
&\frac{E_T}{E} = \frac{1000 - T}{6T - 2800} \quad 600^{\circ}C \le T \le 1000^{\circ}C,
\end{aligned} \tag{5}$$

where $E_T/E = 1000 - T/6T - 2800E_T$ represents the elastic modulus of steel at temperature T ($\mathrm{N/mm^2}$) and E represents the elastic modulus of steel at room temperature ($\mathrm{N/mm^2}$).

2.5. Heat Transfer Principle of a Steel Structure under Fire. When the outside temperature is too high or a fire occurs, the steel structure mainly realizes heat exchange through the outside air and the steel surface to complete heat transfer. The heat transfer inside the structure is realized by the thermal conduction capacity of the steel body [13–15]. Therefore, in the analysis process with the ANSYS software, the temperature load will be transmitted according to the following three channels.

2.5.1. Thermal Conduction. The meaning of thermal conduction of steel is the process that the steel body transfers energy from a high-temperature environment to a low-temperature environment [16]. In this process, heat transfer needs to be completed through contact. This thesis mainly studies the contact between universal beam and beam flange, universal beam and bolt, and universal beam and side column. In addition, the heat transfer calculation among components shall be completed in strict accordance with the following equation:

$$\frac{Q}{t} = \frac{kA(T_2 - T_1)}{d}, \tag{6}$$

where k represents the thermal conductivity of the material. Q is the heat transferred between objects in t time. T represents the external temperature of the material. A represents the surface area of the material. d represents the distance between two objects when completing heat transfer [17].

2.5.2. Thermal Convection. The meaning of thermal convection is the heat transfer process that occurs when the object surface contacts with other fluids under different temperature conditions. This thesis will analyze the heat exchange between air and steel frame surfaces. Equation (7) is to calculate thermal convection:

$$Q = h(T_1 - T_2), \tag{7}$$

where h represents the heat transfer coefficient of the object, T_1 represents the temperature of the external fluid, and T_2 represents the temperature of the object's own surface after contact with the fluid.

2.5.3. Thermal Radiation. Thermal radiation is the heat transfer of objects through electromagnetic waves. As long as the object has temperature, the object will continuously radiate heat energy [18].

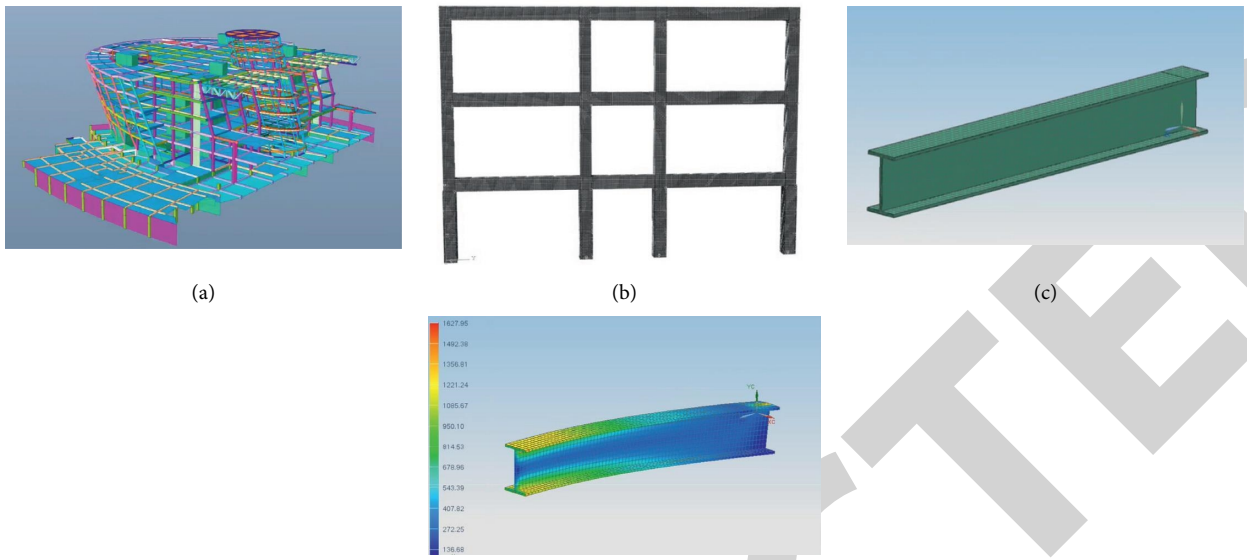

(a) (b) (c) (d)

Figure 1: Finite element analysis model. (a) multistory and high-rise steel structure model; (b) grid division of reinforced concrete frame strengthened with local universal beam; (c) local universal beam model; (d) local universal beam grid.

$$Q = \varnothing \cdot \varepsilon_r \cdot 5.67^{-8} \cdot \left[\left(T_g + 273\right)^4 - \left(T_b + 273\right)^4\right], \quad (8)$$

where $\varnothing$ represents the component shape coefficient, which is usually 1.0. T_g and T_b represent the temperature of steel components, and Q represents the heat transferred from air to steel in unit time; ε_r represents the radiation coefficient.

2.6. Establishment of Finite Element Model. A three-story and three-span reinforced concrete plane frame is taken as the research object. The Abaqus software performs the finite element analysis and calculation of the local frame. Figure 1 shows the finite element analysis model of the steel structure.

ISO834 standard temperature rise curve is adopted. The bottom floor of the frame is under fire, the bottom side column is under fire on three sides, the middle column is under fire on four sides, and the lower part of the bottom beam is under fire [19]. The convective heat transfer coefficient of the fire surface is 25, and the comprehensive radiation coefficient is 0.5; the heat transfer coefficient of heat convection of nonfire surface is 9; the comprehensive radiation coefficient is 0.

In the temperature field analysis, cement mortar and concrete are simulated by DC3D8 element, the steel bar is simulated by DC1D2 element, and angle iron and gusset plate are simulated by DS4 element. Tie constraints are adopted between concrete and concrete, between steel bar and concrete, between angle iron and concrete, between concrete and cement mortar, and between gusset plate and angle iron, regardless of the thermal resistance and slip between contact surfaces.

During mechanical analysis, cement mortar and concrete are simulated by the C3D8R element, the steel bar is simulated by the T3D2 element, and angle iron and gusset plate are simulated by the S4R element [20]. Regardless of the mechanical action of the cement mortar protective layer, tie constraints are adopted between concrete beams and columns and sliding action is considered between angle iron and concrete columns. The contact surface between structural steel and concrete is defined as hard contact in the normal direction and classical Coulomb friction in the tangential direction. The friction coefficient is 0.3, and separation after contact is allowed. The steel bar cages of beams and columns are embedded into beams and columns by means of embedded constraints. It is assumed that there is complete coupling between reinforced joints and concrete joints. Equation (9) is to calculate the axial compression ratio of the steel body:

$$n = \frac{N_c}{\left(f_{ck}A\right)}. \quad (9)$$

where Nc represents the axial load of the calculated section, f_{ck} is the standard value of concrete compressive strength, and A is the section area of the concrete column. Equation (10) is the load ratio:

$$m = \frac{P_0}{P_u}, \quad (10)$$

where P_0 represents the axial force of the column under the frame under the normal temperature environment, and P_u represents the ultimate bearing capacity of the steel structure frame column under the normal temperature environment.

3. Analysis of Experimental Results

3.1. Temperature Field Analysis. Figure 2 shows the comparison of temperature field analysis results.

The change curve in Figure 2(a) suggests a certain difference between the finite element analysis results and the

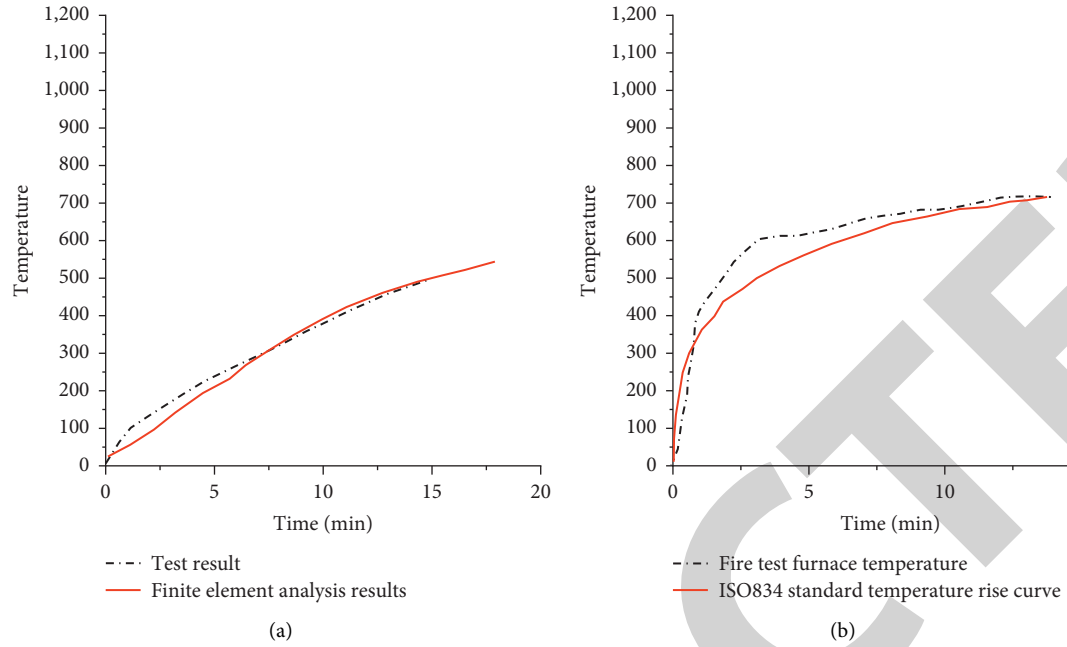

Figure 2: Comparison of temperature field analysis results. (a) Comparison between finite element analysis results and test results; (b) comparison between ISO834 standard temperature rise curve and test furnace temperature.

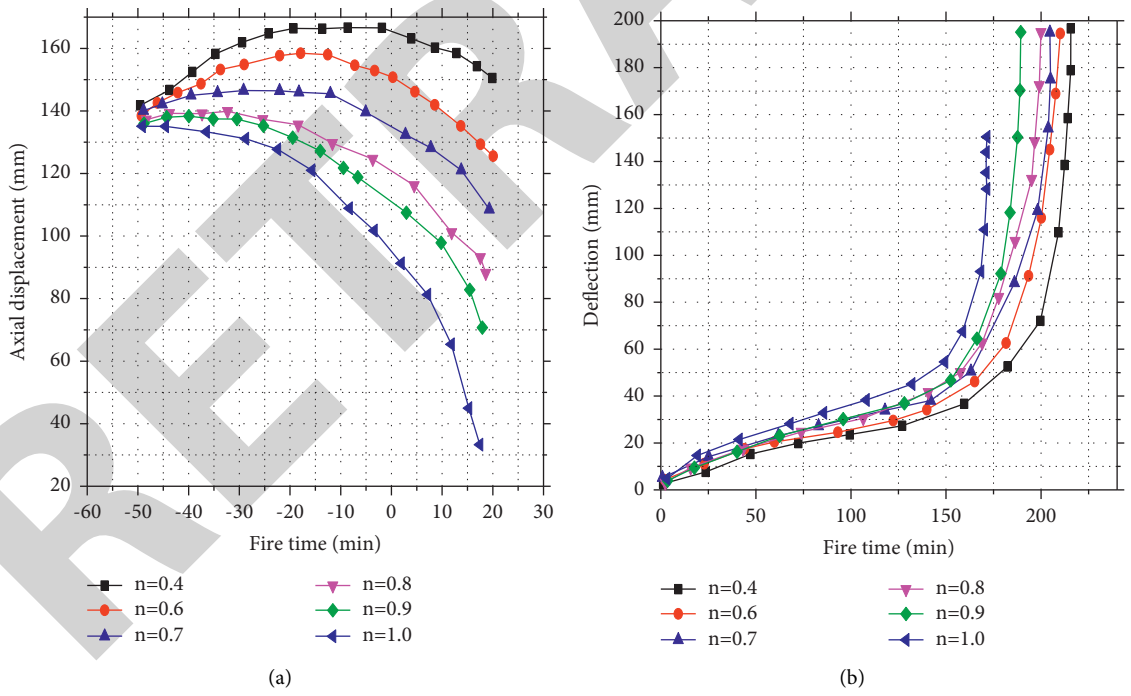

Figure 3: Analysis of axial compression ratio results. (a) Axial displacement analysis diagram of column top in the fire; (b) deflection of side span on fire.

test results within 5 minutes after the fire. However, this difference gradually decreases with the increase of fire time, and finally the two change curves tend to be consistent. In Figure 2(b), within three minutes of the fire, the ISO834 temperature rise curve is lower than the test temperature, and the gap between them gradually increases. At the seventh minute after the fire, the gap gradually decreases. During the subsequent temperature rise, the two curves are almost close. It means that the ANSYS software has good calculation ability in simulating the temperature field of steel

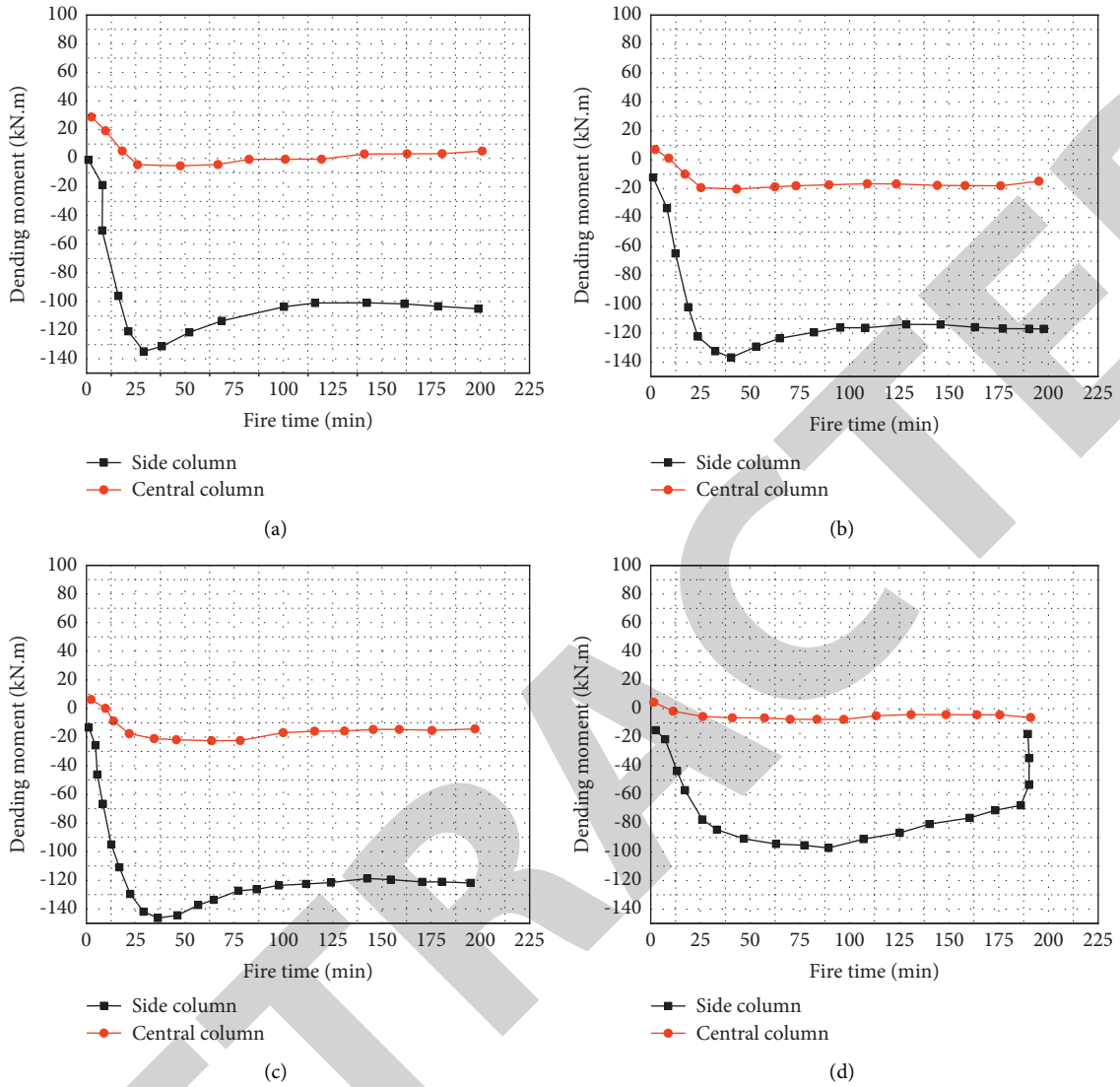

Figure 4: Variation of bending moment at the bottom of the reinforced column under different axial compression ratios. (a) Axial compression ratio $n = 0.4$; (b) axial compression ratio $n = 0.6$; (c) axial compression ratio $n = 0.8$; (d) axial compression ratio $n = 1.0$.

structure and steel beam-column. The test results are basically close to the calculation results.

3.2. Influence Analysis of Axial Compression Ratio. Figure 3 is the result of the axial compression ratio of the steel body.

The result data in Figure 3(a) reveal that when the axial compression ratio is 0.4, 0.6, 0.7, 0.8, and 0.9, the displacement change rate of the column top in the vertical direction is generally small. When the axial compression ratio increases gradually, the transverse deformation rate of the steel body will increase gradually. When the axial compression ratio is 1.0 and the fire time of the steel body is 180 min, the deformation speed of the whole middle column and side column in the vertical direction will increase rapidly. Figure 3(b) proves that there is no obvious difference in the initial fire of steel beams and columns when different axial compression ratios are loaded. The reason is that the deflection of the steel beam itself is affected by its load level, and the influence of the steel beam-column on the steel beam is not very obvious. However, when the axial compression ratio is 1.0 and the fire time is 135 min, the deflection of the steel beam decreases rapidly because the fire resistance of the steel beam and column has reached the limit. Figure 4 shows the bending moment analysis of the bottom end of the reinforced column under different axial compression ratios.

Figure 4 suggests that the bending moment change of the middle column is much smaller than that of the side column bottom because the steel beam restrains each joint of the middle column. When the axial compression ratio is 0.4, 0.6, and 0.8, the bending moment at the bottom of the side column of the whole frame basically has the same change trend. At the beginning of the fire, the growth rate is fast. When the fire time increases, the rate also decreases

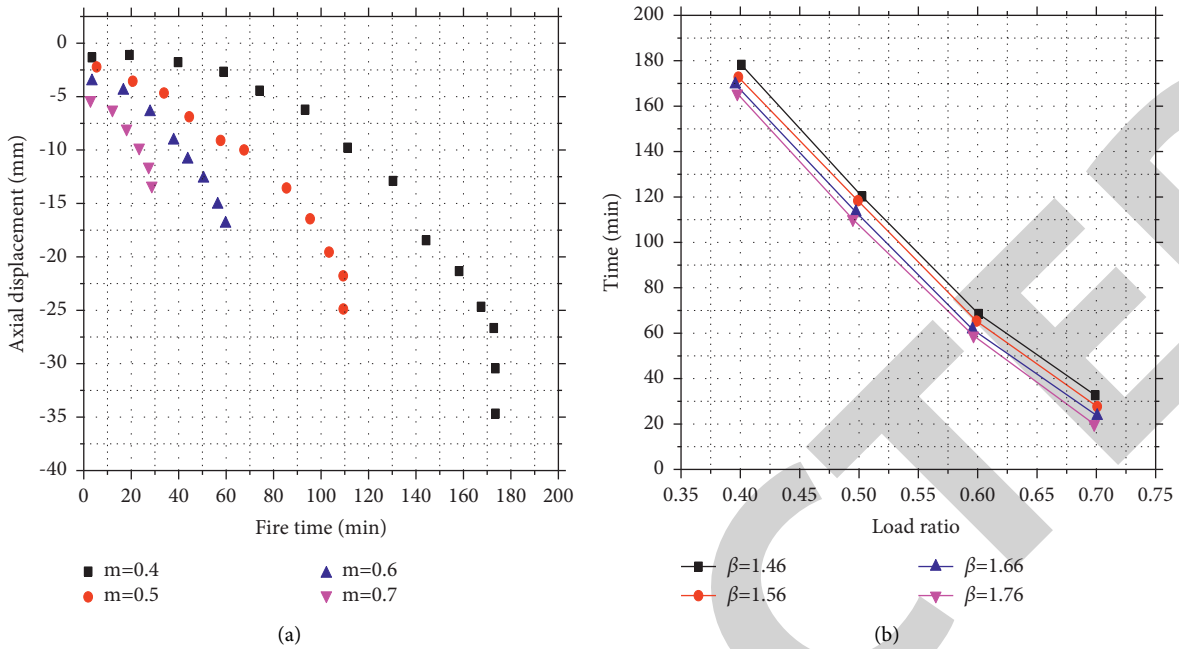

Figure 5: Analysis results of different load ratios of steel body. (a) Variation diagram of lateral displacement of middle column top when the bottom layer is in the fire; (b) fire resistance rating curve of steel frame under different load ratios.

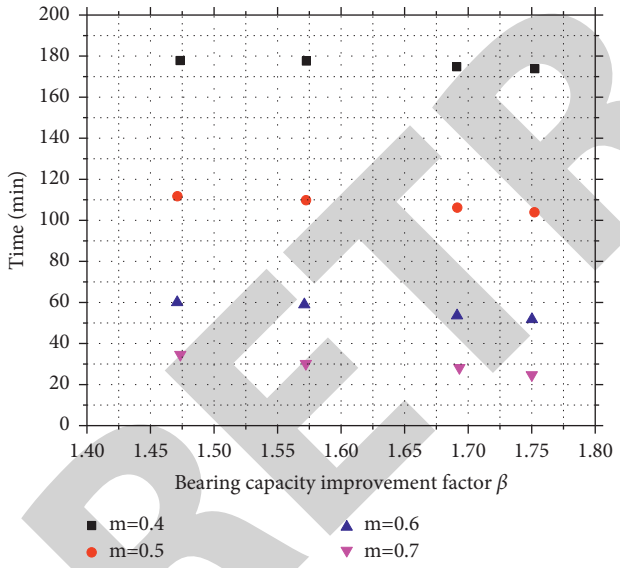

Figure 6: The effect of different bearing capacities on the fire resistance of the steel body.

gradually. When the axial compression ratio is 1.0, the bending moment at the bottom of the side column of the frame increases inversely. It is because the temperature of the steel body increases gradually with the increase of fire time. In the later stage, when the fire time reaches 190 min, the deflection of the beam reaches the maximum, resulting in the tension of the side column to the frame.

3.3. Influence Analysis of Load Ratio. Figure 5 shows the analysis results of different load ratios of the steel body.

The result data in Figure 5(a) show that the axial deformation of the universal beam is obvious under different fire load ratios. When the load ratio increases, the maximum fire resistance of the universal beam will decrease rapidly. Figure 5(b) reveals that when the load ratio increases, the fire resistance of the steel body shows a linear downward trend.

3.4. Influence Analysis of Bearing Capacity Improvement Coefficient. Figure 6 shows the effect of different bearing capacities on the fire resistance of the steel body.

Figure 6 shows that when the steel body is subjected to the same load ratio, different bearing capacities β have little effect on the fire resistance limit of the steel body. It is because the steel itself has good thermal conductivity, and the steel surface has a protective layer, which will make the impact on the steel body when the heat is transferred from the surface to the concrete almost negligible. Therefore, when the whole steel frame is in the same temperature field, the fire resistance of each column is basically the same.

4. Conclusion

The purpose is to analyze the mechanical properties of fabricated multistory and high-rise steel structures and steel beam-column joints after the fire. The thermal performance analysis of steel support is supplemented to improve the comprehensiveness of the research conclusion. First, the thermal and mechanical properties of steel are understood through theoretical research, including thermal conductivity, the thermal expansion coefficient of steel, yield strength, and elastic modulus of ordinary steel. Next, the thermal conduction principle of steel under fire environment is analyzed, including thermal conduction, thermal

convection, and thermal radiation. Then, a three-story and three-span reinforced concrete is selected as the experimental object. The local frame calculation model is established through the finite element software Abaqus. The experimental results show that the middle column of steel frame must be smaller than the side column. It leads to the binding force of the side column is smaller than that of the middle column, and its deformation degree in the horizontal and vertical directions is greater than that of the middle column. When the axial compression ratio of steel increases, the bottom column of the frame deforms first, resulting in the deformation of the whole frame. It suggests that the axial compression ratio can affect the internal force distribution of steel structure frames and the stiffness of steel struts. Finally, the research results of load ratio show that when the load ratio is the same, different bearing capacities β have little effect on the fire resistance limit of the steel body. However, there are some research limitations. For example, there are many joint types in steel structure and steel beam-columns, and the joint type studied is relatively single. Therefore, future related research should focus on targeted analysis on different types of joints. It is hoped that it can provide a reference for relevant teams engaged in steel construction and further reduce the property loss caused by house building fires in the future.

Data Availability

The data used to support the findings of this study are available from the corresponding author upon request.

Conflicts of Interest

The authors declare that they have no conflicts of interest.

References

[1] A. Rezaeian and M. Eskandari, "Effect of temperature on mechanical properties of steel bolts," *Journal of Materials in Civil Engineering*, vol. 32, no. 9, pp. 12–14, 2020.

[2] H. Liu, Y. Zhao, L. Wang, and Z. Chen, "Axial compression properties of welded hollow spherical joints with H-beams under high temperature," *Journal of Constructional Steel Research*, vol. 169, Article ID 106051, 2020.

[3] E. E. Anike, M. Saidani, A. O. Olubanwo, M. Tyrer, and E. Ganjian, "Effect of mix design methods on the mechanical properties of steel fibre-reinforced concrete prepared with recycled aggregates from precast waste," *Structures*, vol. 27, pp. 664–672, 2020.

[4] B. K. Cirpici, "Design analysis of a steel industrial building with wide openings exposed to fire," *Challenge Journal of Structural Mechanics*, vol. 6, no. 3, 2020.

[5] R. Chan, C. Moy, and I. Galobardes, "Factor affecting the bond quality of functionally graded concretes produced with steel fiber and recycled aggregates," *Materials and Structures*, vol. 54, no. 4, pp. 16–18, 2021.

[6] J. Ahmad, A. Manan, A. Ali, M. W. Khan, M. Asim, and O. Zaid, "A study on mechanical and durability aspects of concrete modified with steel fibers (SFs)," *Civil Engineering and Architecture*, vol. 8, no. 5, pp. 814–823, 2020.

[7] C. Yu, W. Ding, T. Wu, and Q. Zhang, "Study on calculation method of new corrugated steel reinforcement structure of highway tunnel," *IOP Conference Series: Materials Science and Engineering*, vol. 741, no. 1, Article ID 012073, 2020.

[8] S. Chang, M. Yang, L. Tian, and P. Yuan, "Bending behavior of steel octagon-web beam," *Advances in Structural Engineering*, vol. 23, no. 12, pp. 2694–2708, 2020.

[9] R. Huang, S. Li, L. Meng, D. Jiang, and P. Li, "Coupled effect of temperature and strain rate on mechanical properties of steel fiber-reinforced concrete," *International Journal of Concrete Structures and Materials*, vol. 14, no. 1, pp. 21–24, 2020.

[10] X. Cui and X. Ling, "Effects of differential subgrade settlement on damage distribution and mechanical properties of CRTS II slab track," *Construction and Building Materials*, vol. 271, no. 1, Article ID 121821, 2021.

[11] P. K. Deshpande, K. K. Sangle, and Y. M. Ghugal, "Synergistic effect of SBR latex and steel fibres on mechanical properties of high strength concrete," *Journal of Structural Engineering*, vol. 47, no. 3, pp. 259–268, 2020.

[12] J. Xu, W. Wang, and Q. Han, "Mechanical properties of pultruded high-temperature-resistant carbon-fiber-reinforced polymer tendons at elevated temperatures," *Construction and Building Materials*, vol. 258, Article ID 119526, 2020.

[13] T. Bahtli and N. S. Ozbay, "Mechanical properties and freeze-thaw resistances of bronze-concrete composites," *Challenge Journal of Concrete Research Letters*, vol. 12, no. 2, 2021.

[14] G. D. Lorenzo, A. Formisano, G. Terracciano, and R. Landolfo, "Iron alloys and structural steels from XIX century until today: evolution of mechanical properties and proposal of a rapid identification method," *Construction and Building Materials*, vol. 302, no. 8, Article ID 124132, 2021.

[15] X. Guo and X. Pan, "Effects of steel slag on mechanical properties and mechanism of fly ash–based geopolymer," *Journal of Materials in Civil Engineering*, vol. 32, no. 2, 2020.

[16] Z. Cao and L. Xiao, "Fire resistance characteristics of steel-concrete-steel structure and reinforced concrete structure in an eight-lane dual-directional super large-span immersed tunnel," *IOP Conference Series: Materials Science and Engineering*, vol. 838, no. 1, Article ID 012010, 2020.

[17] T. Zhang, J. Lu, L. Sun et al., "Mydriasis-free flicker electroretinograms in 204 healthy children aged 0-18 Years: reference data from two cohorts," *Translational vision science & technology*, vol. 10, no. 13, p. 7, 2021.

[18] N. A. Khudhair and A. Al-Sammarraie, "Study the effect of SiO 2 nanoparticles as additive on corrosion protection of steel rebar in artificial concrete solution," *Journal of Engineering and Applied Sciences*, vol. 14, no. 9, pp. 2-3, 2020.

[19] Y. Li, Y. Shao, and X. Wang, "Finite element analysis of mechanical performance of concrete-filled steel tube composite frame under different fire time," *E3S Web of Conferences*, vol. 257, no. 12, Article ID 01086, 2021.

[20] V. Tahouneh, M. H. Naei, and M. M. Mashhadi, "Influence of vacancy defects on vibration analysis of graphene sheets applying isogeometric method: molecular and continuum approaches," *Steel and Composite Structures*, vol. 34, no. 2, pp. 261–277, 2020.